

# Cryptic variations of minor elements Al, Cr, Ti and Mn in Lower and Critical Zone orthopyroxenes of the Western Bushveld Complex

H. V. EALES, B. TEIGLER AND W. D. MAIER

Department of Geology, Rhodes University, Grahamstown, South Africa

## Abstract

Compositional variations with respect to minor elements Al, Cr, Ti and Mn, and major elements Fe and Mg, in orthopyroxenes along *ca.* 160 km of strike of the Lower (LZ), Lower Critical (LCZ) and Upper Critical (UCZ) Zones are reviewed on the basis of 1900 analyses by electron microprobe. Al increases with stratigraphic height and declining Mg/(Mg + Fe<sup>2+</sup>) ratios (hereafter MMF ratios) through the LZ and LCZ, reaching peak values close to the base of the UCZ, where the first cumulus plagioclase appears in the succession. Above this, Al contents decline as MMF ratios decline. Through the same interval, subdued increase in Ti occurs through >1000 m of ultramafic cumulates, but this increase accelerates within the *ca.* 450 m UCZ sequence. Mn increases linearly with declining MMF ratios through the entire succession. Cr levels are highest in orthopyroxenes of the ultramafic LZ and LCZ, and olivine norites of the UCZ, but decline in more evolved norites and associated anorthosites of the UCZ.

This pattern of cryptic variations, displayed by a thick succession of cumulates, is consistent with the model of Bence and Papike (1972) and Grove and Bence (1977) for basaltic rocks, which links the levels of minor elements in pyroxenes with entry of plagioclase into the paragenesis.

**KEYWORDS:** orthopyroxene, Bushveld complex, pyroxenites, norites, anorthosites.

## Introduction

COMPOSITIONAL variations of pyroxenes in basaltic rocks have been shown by Bence and Papike (1972) to be a function of the order of crystallisation, which these authors link in turn to different bulk compositions, emplacement histories, *P*, *T* and *f*<sub>O<sub>2</sub></sub>. Where plagioclase is not a liquidus phase in the early stages of crystallisation, pyroxenes are enriched in Al, and display low Ti/Al ratios. With the onset of plagioclase crystallisation, Al in pyroxenes declines and Ti/Al ratios increase sharply, by virtue of the incompatibility of Ti in plagioclase. Experimental studies on melts (Grove and Bence, 1977) have emphasised that major-element partitioning between liquid and pyroxenes is essentially independent of cooling rate, but partitioning of minor elements is sensitive to different lines of liquid descent. Ion microprobe studies by Shearer *et al.* (1989) have broadened this concept by tracing

variations of REE and other trace elements in pyroxenes of basalts in which plagioclase nucleation was delayed to different degrees. Like Al, Na is enriched in basaltic pyroxenes where plagioclase is suppressed, but declines with increasing Ti/Al ratios where suppression is less marked.

These relationships stress the importance of pyroxene chemistry, both because of its prolonged period of growth in basaltic melts, and because minor elements may reflect the paragenetic sequence of the host rocks. The present paper uses orthopyroxene microprobe data to test whether these principles have application to cumulates of the Bushveld layered complex. Here the paragenetic sequence is chromite–olivine–orthopyroxene–plagioclase–clinopyroxene. In the Lower and Critical Zones, clinopyroxene is almost exclusively a late, intercumulus or poikilitic phase and its cryptic variations are of no significance in the present context. The emphasis here is on compositional evolution of the ortho-

pyroxene with stratigraphic height, and the differences in its compositional trends prior, and subsequent, to the appearance of plagioclase as a cumulus phase.

### Orthopyroxenes of the Bushveld Complex

*Analytical methods.* All samples were analysed for Si, Ti, Al, Cr, Fe, Mn, Ni, Mg, Ca and Na, using a JEOL CXA-733 Superprobe. The same standards and procedures were retained throughout, the analyses of the core domains of up to 12 cumulus crystals were averaged to derive representative data for each sample. The data yield an average of 3.999 cations per six oxygens, and an average charge deficit ( ${}^{\text{iv}}\text{Al} + \text{Na}$ ) - ( ${}^{\text{vi}}\text{Al} + \text{Cr} + 2\text{Ti}$ ) of  $-0.0010$ , indicating a trivial role for  $\text{Fe}^{3+}$  (Cameron and Papike, 1981).

Fine-scale exsolution of clinopyroxene from orthopyroxene is ubiquitous, hence minor variation in relative volumes of the two phases encompassed by the  $10\ \mu\text{m}$  defocussed electron beam is unavoidable. This has no significant effect on the determination of Si, Ti, Al, Cr and Mn. Average intra-sample coefficients of variation (100 std. dev./mean) are 0.38% for Si, and 1% for Mg, but higher for minor elements (Al: 7.2%). Being *ca.* 15 times more abundant in clinopyroxene than in orthopyroxene, Ca shows high coefficients (*ca.* 21%), and Ca data for orthopyroxenes are regarded as unreliable. In practice, the rare analyses with  $\text{CaO} > 2\%$  were rejected.  $\text{Na}_2\text{O}$  is invariably  $< 0.05\%$ . Representative averages are given in Table 1, for the six groups of samples into which the population is split (see Fig. 1). Si, Mg and Cr decline progressively through Groups A-F, while, Fe, Mn and Ti increase.

*Sample selection.* The Bushveld Complex is divisible on lithology into a Lower Zone (hereafter LZ) dominated by dunites, harzburgites and orthopyroxenites, Lower Critical Zone (LCZ) of mainly orthopyroxenites and chromitiferous layers, Upper Critical Zone (UCZ) where cumulus plagioclase joins the paragenesis to add norites and anorthosites to the assemblage, Main Zone of gabbro-noritic and leucocratic rocks, and Upper Zone distinguished by cumulus magnetite, fayalitic olivine and apatite. The succession is *ca.* 7 km thick in the western limb of the complex.

Fig. 1 illustrates the stratigraphic interval under review, and the sample groupings adopted for this paper. In view of the regional changes in petrography and chemistry of the rocks of the western limb (Eales *et al.*, 1988; Teigler, 1990; Maier, 1991; de Klerk, 1991; Teigler *et al.*, 1992) norites are here further segregated into those of a western or proximal facies, and those of an

eastern or distal facies. This concept of facies variation correlates increasing distance from the Union Section (proximal) area with features such as the progressive thinning of individual chromitite and olivine-rich layers in the LCZ, progressive decline in the MMF ratios of both olivine and orthopyroxene in cumulates, and progressive thickening (35 m to  $> 200$  m) and increase in the modal proportion of plagioclase ( $< 40\%$  to  $> 75\%$ ) of the interval between the Merensky Reef and UG1 chromitite of the UCZ, as well as other gradational changes. The strike-length separating the proximal facies, centred in R.P.M. Union Section Mine, and the most distal exposures in the Brits graben, is *ca.* 160 km (a locality map is available in Viljoen and Hieber, 1986, p. 1108). The groups adopted are:

Group F: anorthosites in the uppermost part of the UCZ (between UG2 and Merensky Units);  
Group E: UCZ norites within the same stratigraphic interval as above (distal facies);

Group D: norites, as above, but in the western or proximal facies;

Group C: orthopyroxenites straddling the UCZ/LCZ boundary (35 m below to 70 m above boundary);

Group B: orthopyroxenites of the upper third of the LCZ (35 m to 285 m below UCZ/LCZ boundary); and

Group A: orthopyroxenites of the lower 500 m of the LCZ and uppermost 300 m of the LZ.

Of 336 samples covering the indicated stratigraphic interval, 30 (8.9%) have been rejected on the grounds of anomalous composition (conceivably related to the proximity of mafic pegmatites), or indication of sub-solidus reaction with chromite (exceptionally high MMF ratios). Patterns of cryptic variation indicated by the remaining 306 samples (91%; 1900 analyses) are illustrated in Figs. 2-6, with the field boundaries drawn to enclose all datum points.

*MnO vs. MMF ratios.* The plot of MnO vs. Mg/(Mg + Fe<sup>2+</sup>) ratio (hereafter MMF ratio) is shown in Fig. 2 to define an inverse linear relationship, with MnO ranging from *ca.* 0.14% in the LZ to  $> 0.4\%$  near the roof of the UCZ. There is an overlap of fields A-F, which emphasises the continuity of the trend, and an absence of inflections. The Mn content is, therefore, closely linked to the Fe content.

*Al<sub>2</sub>O<sub>3</sub> vs. MMF Ratio.* Fig. 3 charts the general increase in total Al<sub>2</sub>O<sub>3</sub> with increasing stratigraphic height through the LZ and LCZ, as the general tenor of MMF ratios declines through Groups A-C. Peak values of *ca.* 1.5% Al<sub>2</sub>O<sub>3</sub> in pyroxenites are attained at the LCZ/UCZ bound-

TABLE 1

Averaged Compositions of Orthopyroxenes of Groups A - F

	A	B	C	D	E	F
SiO <sub>2</sub>	56.19	55.73	55.28	55.00	54.83	53.79
TiO <sub>2</sub>	0.071	0.100	0.134	0.161	0.201	0.256
Al <sub>2</sub> O <sub>3</sub>	1.112	1.224	1.237	1.294	1.034	0.836
Cr <sub>2</sub> O <sub>3</sub>	0.475	0.473	0.461	0.426	0.384	0.191
FeO	9.32	10.77	11.67	12.61	13.54	18.33
MnO	0.205	0.233	0.243	0.259	0.279	0.363
NiO	0.07	0.08	0.08	0.09	0.09	0.08
MgO	31.12	29.81	29.53	28.95	28.27	24.93
CaO	1.27	1.28	1.23	1.22	1.32	1.05
Na <sub>2</sub> O	0.03	0.02	0.01	0.02	0.02	0.01
Totals	99.85	99.72	99.88	100.03	99.95	99.95
Si	1.9739	1.9736	1.9642	1.9603	1.9650	1.9718
Ti	0.0018	0.0026	0.0035	0.0043	0.0054	0.0070
Al	0.0460	0.0510	0.0518	0.0543	0.0436	0.0361
Cr	0.0131	0.0132	0.0129	0.0120	0.0108	0.0055
Fe	0.2740	0.3189	0.3468	0.3759	0.4057	0.5619
Mn	0.0061	0.0069	0.0073	0.0078	0.0084	0.0112
Mg	1.6291	1.5734	1.5634	1.5377	1.5096	1.3623
Ca	0.0476	0.0487	0.0468	0.0465	0.0505	0.0410
Na	0.0017	0.0014	0.0009	0.0011	0.0011	0.0009
Ni	0.0019	0.0021	0.0021	0.0025	0.0022	0.0024
Cations	3.9954	3.9922	4.0002	4.0027	4.0028	4.0006
Charge	-0.009	-0.015	0.001	0.006	0.006	0.002
MMF	0.856	0.832	0.818	0.804	0.788	0.708
n	85	32	18	58	93	20

Stratigraphic intervals covered by Groups A - F are shown in Fig. 1 and discussed in text. 'n' represents number of samples; MMF is  $Mg/(Mg+Fe^{2+})$ ; 'cations' are calculated for 6 oxygens; 'charge' is  $(^{iv}Al+Na)-(^{vi}Al+Cr+2Ti)$ .

ary (Group C), where cumulus plagioclase first appears. A further increase to >1.6% manifests itself in the more primitive norites and olivine norites of the proximal facies (Group D), following which there is a virtually linear decrease through the more evolved distal norites (Group

E) and anorthosites (Group F). Pyroxenes of anorthosites are intercumulus in habit, and at low MMF ratios of 0.62, Al<sub>2</sub>O<sub>3</sub> contents decline to <0.8%.

While there is overlap between fields A-F, there is clearly (a) overall increase in Al from low

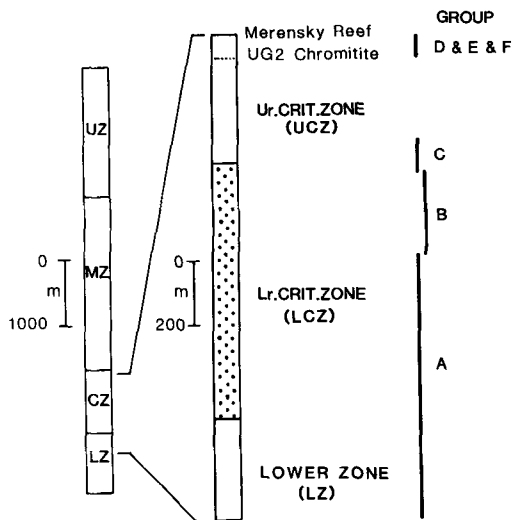


FIG. 1. Simplified stratigraphic profile of the Bushveld Complex, showing sample groupings A–F. UZ—Upper Zone; MZ—Main Zone; CZ—Critical Zone; LZ—Lower Zone.

values within the primitive members lower in the cumulate pile, (b) an inflection near the LCZ/UCZ boundary, and (c) subsequent decline with fractionation towards Fe-enriched members.

A second-order variation appears to be superimposed on the trends established above. It is known that the Bushveld Complex displays megacyclicity in terms of variations of the MMF ratio, attributed to periodic addition of fresh, hot magma to the chamber (Teigler, 1990; Eales *et al.*, 1990b). Such megacycles are 50–300 m

thick in the LZ and LCZ, with prolonged reversals of the normal fractionation trend culminating in cappings of olivine-rich cumulates. If the data points of Groups A–C are regrouped so as to represent three stratigraphic intervals dominated by normal fractionation trends (decreasing MMF ratio) as in Fig. 3d, it becomes apparent that a second-order trend exists, oblique to the gross trend of increasing Al with declining MMF ratio. That is, within limited stratigraphic intervals, a positive correlation persists between Mg and Al contents of the orthopyroxene. This is the normal pattern for orthopyroxenes of metaluminous igneous rocks, established by Maeda *et al.* (1991) and attributed to temperature control. This would be consistent with microprobe studies of zoning in orthopyroxene grains (Teigler, 1990; Maier, 1991) which show that depletion of Al towards crystal margins is the norm for all Bushveld lithologies.

$TiO_2$  vs.  $Al_2O_3$ . The progressive decline in averaged MMF ratios through Groups A–F (Fig. 3) is matched in Fig. 4a by progressive increase in the incompatible element Ti. Pyroxenites of Group A constitute a compact grouping indicating little compositional change through the lowermost 800 m of section. Both Al and Ti (Fig. 4b–d) rise through Groups B–C, spanning some 350 m of section. Average levels of Ti are thus roughly doubled through the lower 1150 m of section. Following the appearance of plagioclase as a cumulus phase, Ti in orthopyroxene is more than doubled again through the relatively thin interval spanned by Groups D–F in the UCZ (*ca.* 400 m in the Union Section area). Concomitantly, Al declines by close on 50% through the same interval. Averaged Ti/Al ratios, from the data on

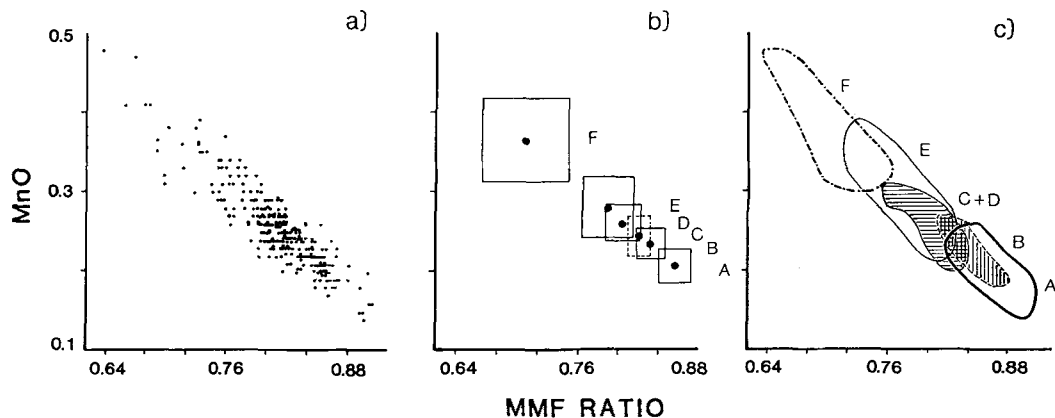


FIG. 2. Plots of per cent MnO versus MMF ratio of orthopyroxenes in 306 samples within Groups A–F. (a) All datum points. (b) Calculated mean values for each of Groups A–F, with boxes representing 1 standard deviation. (c) Field boundaries encompassing all datum points within each of Groups A–F.

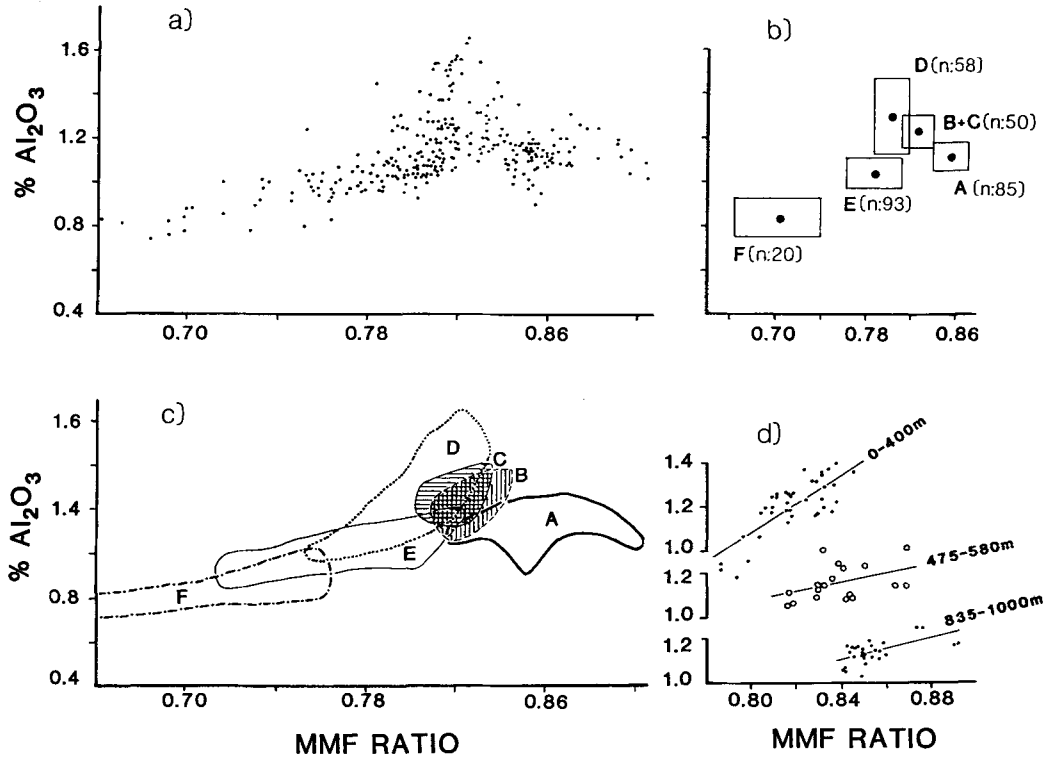


FIG. 3. Plots of per cent  $\text{Al}_2\text{O}_3$  versus MMF ratio of orthopyroxenes in 306 samples within Groups A-F. (a) All datum points. (b) Calculated mean values for each of Groups A-F, with boxes representing 1 standard deviation. (c) Field boundaries encompassing all datum points within each of Groups A-F. (d) Calculated regression lines for limited intervals with the stratigraphic sequence embraced by Groups A-C (see text).

which Fig. 4c is based, are, respectively, 0.072, 0.093, 0.123, 0.141, 0.220 and 0.347 for Groups A-F.

A curve drawn through the computed averages for each group (Fig. 4c) would thus show progressive increase in Ti with height, but pronounced inflection in Al contents some 50–100 m above the level where plagioclase first becomes a cumulus phase. The level at which this inflection occurs is not sharply defined, as the base of the Critical Zone is marked by repeated mixing of fractionated residua with fresh additions of primitive liquid, yielding hybrid liquids (Eales *et al.*, 1990a).

Some analogies may be drawn with the Great Dyke of Zimbabwe. Wilson's (1982) study of >2000 m of section through the Ultramafic Zone (equivalent to the LZ and LCZ of the Bushveld Complex) provides data on orthopyroxenes. His data were derived in part by microprobe analysis, and in part by XRF analysis of mineral separates. Although the latter yielded  $\text{Al}_2\text{O}_3$  contents consistently *ca.* 0.4% higher than microprobe tech-

niques (here plotted in Fig. 5) both techniques revealed a clear increase of Ti as Al of the orthopyroxenes increases, as in equivalent rocks of the Bushveld complex.

$\text{Cr}_2\text{O}_3$  vs.  $\text{Al}_2\text{O}_3$ . Trends defined by Cr are poorly resolved through LZ and LCZ pyroxenites, and the more primitive UCZ norites (Fig. 6). Levels of  $\text{Cr}_2\text{O}_3$  scatter within the range 0.4–0.55%, implying a close approach to saturation. Depletion of Cr, together with Al, is evident in the distal norites, and anorthosites. Orthopyroxenes of anorthosites display consistently low  $\text{Cr}_2\text{O}_3$  contents, 95% of the samples being within the range 0.03–0.3%.

### Summary and discussion

One of the more fundamental changes in lithology of the Bushveld complex occurs at the LCZ/UCZ boundary, where plagioclase becomes a cumulus phase. This boundary is clearly recognisable between the MG2 and MG3 chromitite layers at all places, even although recent work (Teigler *et al.*, 1992) has shown that in the distal

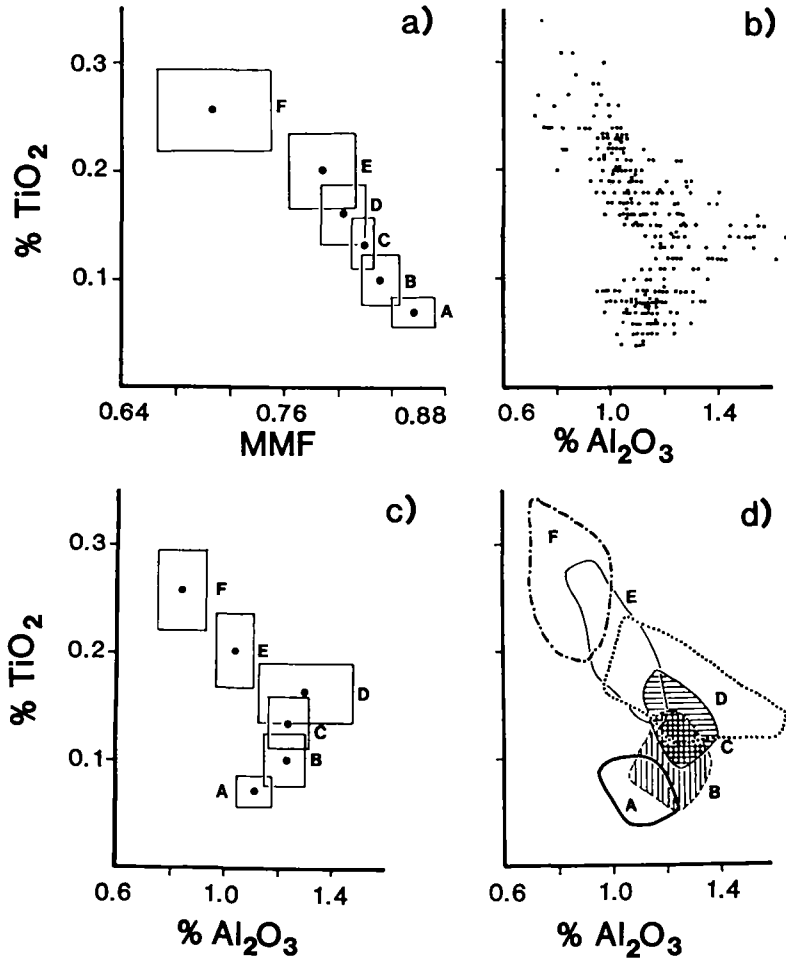


FIG. 4. Plots of per cent TiO<sub>2</sub> versus (a) MMF ratio, with boxes representing 1 standard deviation, and (b)–(d) Al<sub>2</sub>O<sub>3</sub> in orthopyroxenes of 306 samples within Groups A–F. (b) All datum points. (c) Calculated mean values for each of Groups A–F, with boxes representing 1 standard deviation. (d) Field boundaries encompassing all datum points within Groups A–F.

facies, in the vicinity of the Brits graben, cumulus plagioclase enters the LCZ well below the boundary as previously defined.

Data presented here show that fundamentally different patterns of cryptic variation prevail above and below this boundary. In summary, (a) averaged values of Al<sub>opx</sub> increase with stratigraphic height, and overall decline of MMF ratios, through the LZ and LCZ (Fig. 3), but (b) an inflection occurs at the LCZ/UCZ boundary, above which Al<sub>opx</sub> decreases with further decline in MMF ratios; (c) Ti<sub>opx</sub> increases through the same interval (Fig. 4), but an accelerated rate (with reference to the thickness of the interval through which the increase is recorded) after

cumulus plagioclase joins the paragenesis; (d) Mn levels increase sufficiently regularly with declining MMF ratios to provide a rough guide to the rock type, and its level within the complex; and (e) overlap between Groups A–F, as defined earlier, indicates that the evolutionary trends are essentially continuous, without abrupt discontinuities such as might be expected from emplacement of magmas of different lineages.

These patterns of variation are fully consistent with the entry of low, but increasing, levels of Ti and Al into orthopyroxene as the liquids evolved in the earlier stages towards the pyroxene-plagioclase cotectic. This was the overall trend, despite frequent reversals due to injection of

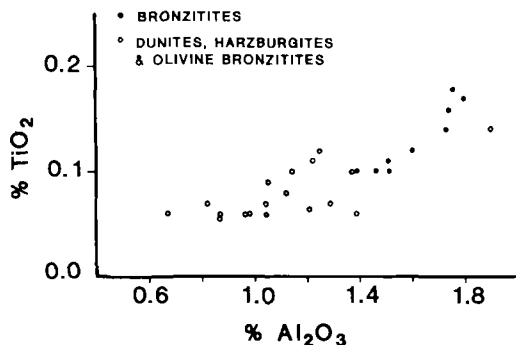


FIG. 5. Plot of  $\text{TiO}_2$  versus  $\text{Al}_2\text{O}_3$  in ultramafic rocks of the Great Dyke of Zimbabwe (data from Wilson, 1982). Data for bronzites derived from whole-rock analysis of mineral separates, and, for remaining rocks, from microprobe analyses.

batches of fresh, primitive liquid into the chamber. On reaching the cotectic, the crystallisation of plagioclase would have initiated depletion of the liquid in Al, while enriching it in the incompatible element Ti. Because Cr is also incompatible with respect to plagioclase, the associated pyroxene was also enriched in Cr; as shown in Fig. 6, the pyroxenes of some of the more primitive norites contain more Cr than those of most pyroxenites, and depletion is evident only in the more evolved distal norites, and in anorthosites.

Cryptic variations in the minor elements of orthopyroxene, through the cumulate sequence,

may therefore be explained by the same model as advanced by Bence and Papike (1972), Grove and Bence (1977), and Shearer *et al.* (1989) in their studies of basaltic rocks, *viz.*, the entry of plagioclase into the paragenesis is reflected in the minor-element chemistry of the pyroxenes. Fundamental control is exerted by the composition of the immediate, parent liquid with which the pyroxene is in contact.

The more highly evolved character of the norites in the distal facies is readily explained in this context. We have pointed out that cumulus plagioclase in the distal facies enters the paragenesis well below the LCZ/UCZ boundary as traditionally defined elsewhere. This early separation of plagioclase has therefore caused the orthopyroxenes to display chemically evolved traits at a deeper stratigraphic level in the distal facies than elsewhere. Accordingly, the compositions of orthopyroxenes of distal norites overlap those of anorthosites of the proximal facies by the stage that the LCZ/UCZ boundary was reached.

The role played by phases other than plagioclase, *i.e.* chromite and olivine, merits brief comment. The foregoing study has specifically excluded from consideration harzburgites and dunites, in which olivine is a major phase. There is more scatter of Al and Ti data in such rocks. In some samples the composition of the orthopyroxene is indistinguishable from that in olivine-poor cumulates occurring at similar stratigraphic levels (Groups A–C of Figs. 2–4 and 6), but in others the data reveal significant enrichment in Ti, or Al, or

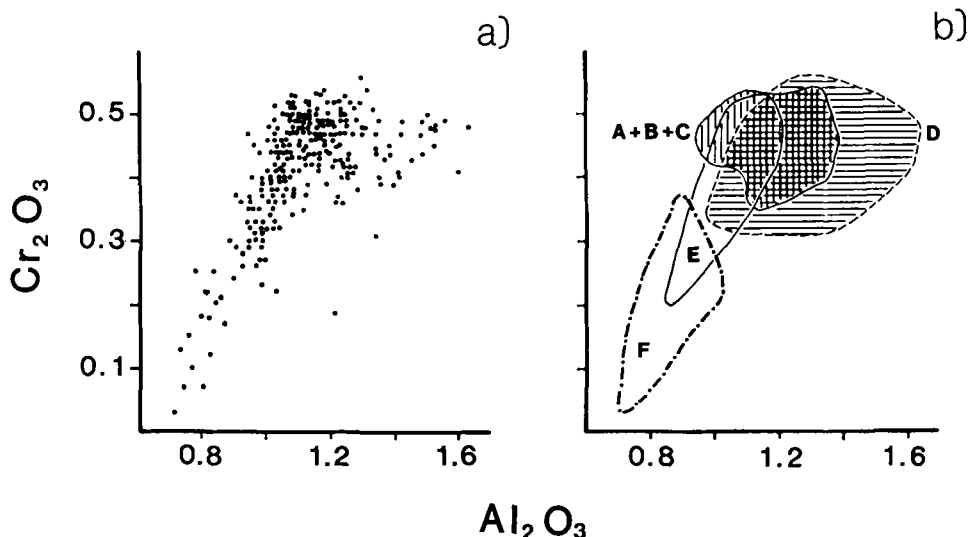


FIG. 6. Plot of  $\text{Cr}_2\text{O}_3$  versus  $\text{Al}_2\text{O}_3$  in orthopyroxenes of 306 samples within Groups A–F. (a) All datum points. (b) Field boundaries encompassing datum points of Groups A–F (Groups A–C are combined for simplicity).

both. This is consistent with the low distribution coefficients for Ti and Al in olivine, the crystallisation of which will enrich the intercumulus liquid in these elements where it is trapped in the cumulates. A systematic study of 123 samples (1230 microprobe analyses; unpublished data) drawn from 17 borehole intersections of the UG2 pyroxenite has established that within 1.25 m of the contact with the underlying UG2 chromitite, the orthopyroxene is depleted, by a factor of *ca.* 0.7, in Cr. Cr/Al ratios are depressed, but Ti/Al ratios are unaffected relative to values in higher levels of the layer. The cumulative thickness of the chromitite layer and its leaders is *ca.* 1 m, and this indicates that even copious crystallisation of Cr-spinel has had only a minor and localised effect on levels of Cr, Al and Ti in orthopyroxene cumulates that succeeded chromitite layers. Of greater genetic significance is the progressive change in composition of Cr-spinel in successive chromitite layers. The data compiled by Teigler and Eales (1991) for 19 successive chromitite layers of the CZ reveal that Ti and Al in the Cr-spinel increase, but Cr declines, with stratigraphic height through the sequence of layers. As Cr-spinel is the earliest phase in the paragenesis, and chromitites occur at the base of many cyclic units, they should reflect evolutionary changes in the composition of the parent liquids in the magma chamber. Sub-solidus reactions should be insignificant in the massive layers, and therefore the trends of the increase of Ti and Al with stratigraphic height of the evolving liquids, deduced from orthopyroxene data, are confirmed by the spinel data.

#### Acknowledgements

The South African Foundation for Research Development is thanked for financial support of all three authors in previous years. The managements of J.C.I. Ltd, Rand Mines Ltd, and Genmin Ltd, are thanked for allowing us access to sample material. The co-operation of Rob Skae was invaluable during the compilation of the microprobe data.

#### References

Bence, A. E. and Papike, J. J. (1972) Pyroxenes as recorders of lunar basalt petrogenesis. *Proc. Third Lunar Sci. Conference*, 431–69.  
Cameron, M. and Papike, J. J. (1981) Structural and

chemical variation in pyroxenes. *Amer. Min.*, **66**, 1–50.  
De Klerk, W. J. (1991) *Petrology and geochemistry of the upper Critical Zone in the Western Bushveld Complex*. Unpubl. Ph.D. thesis, Rhodes University, 294 pp.  
Eales, H. V., Field, M., de Klerk, W. J., and Scoon, R. N. (1988) Regional trends of chemical variation and thermal erosion in the Upper Critical Zone, Western Bushveld Complex. *Mineral. Mag.*, **52**, 63–79.  
— de Klerk, W. J., Butcher, A. R., and Kruger, F. J. (1990a) The cyclic unit beneath the UG1 chromitite at R.P.M. Union Section Mine. *Ibid.*, **54**, 23–43.  
— and Teigler, B. (1990b) Evidence for magma mixing processes within the Critical and Lower Zones in the northwestern Bushveld Complex. *Chem. Geol.*, **88**, 261–78.  
Grove, T. L. and Bence, A. E. (1977) Experimental study of pyroxene–liquid interaction in quartz-normative basalt. *Proc. Eighth Lunar Sci. Conference*, 1549–79.  
Maeda, J., Shimura, T., Arita, K., Osanai, Y., Murata, M., Bamba, M., and Suetake, S. (1991) Chemical features of orthopyroxene in peraluminous igneous rocks. *Amer. Min.*, **76**, 1674–82.  
Maier, W. D. (1991) *Geochemical and petrological trends in the UG2–Merensky Unit interval, Western Bushveld Complex*. Unpubl. Ph.D. thesis, Rhodes University, 241 pp.  
Shearer, C. K., Papike, J. J., Simon, S. B., and Shimizu, N. (1989) An ion microprobe study of the intra-crystalline behaviour of REE and selected trace elements in pyroxene. *Geochim. Cosmochim. Acta*, **53**, 1041–54.  
Teigler, B. (1990) *Mineralogy, petrology and geochemistry of the Lower and lower Critical Zones, northwestern Bushveld Complex*. Unpubl. Ph.D. thesis, Rhodes University, 247 pp.  
— and Eales, H. V. (1991) Correlation between chromite composition and PGE mineralisation in the Critical Zone of the western Bushveld Complex. *Internat. Congr. Appl. Mineral.* '91, Pretoria, 2, Paper 59.  
— and Scoon, R. N. (1992) The cumulate succession in the Critical Zone of the Rustenburg Layered Suite at Brits, Western Bushveld Complex. *South African J. Geol.*, **95**, 17–28.  
Viljoen, M. J. and Hieber, R. (1986) The Rustenburg Section of R.P.M. Ltd. In *Mineral Deposits of Southern Africa* (C. R. Anhaeusser and S. Maske, Editors), Geol. Soc. South Africa, 1107–34.  
Wilson, A. H. (1982) The geology of the Great 'Dyke', Zimbabwe. *J. Petrol.*, **23**, 249–92.

[Manuscript received 30 March 1992;  
revised 15 June 1992]